



Research Article

Growth, Spectroscopic, Hyperpolarizability and Dielectric studies on 8-Hydroxy Quinolinium Benzoate (8HQB) Crystal

J. Balaji^{1*}, P. Rammivasmirtha²

¹Department of Physics, University College of Engineering: Panruti
(A Constituent College of Anna University, Chennai), Panruti - 607 106. India.

²Department of Chemistry, Cheran College of Engineering, Karur - 639 111. India.

*Corresponding author's e-mail: ramjbalaj@gmail.com

Abstract

An organic Non-linear optical crystal, 8 Hydroxy quinolinium benzoate is grown by slow evaporation technique using ethanol as solvent. Cell parameter for grown crystal is observed from single crystal XRD and the crystal belongs to the centrosymmetric crystal structure with $P2_1/c$ space group. The molecular structure and various functional groups are identified by ¹H NMR, FTIR and FTRaman analysis. The dielectric responses of the compound have been studied in the frequency range 100 Hz–5MHz at various temperatures. The first order hyperpolarizability of 8HQB is computed by Density functional theory using B3LYP/ HF6-31G (d,p) level. The total number of vibrational modes is obtained using factor group analysis. Thermal suitability in optical application is analysed using TG/DTA thermal analysis. The lower cutoff wavelength of grown crystal is 243 nm. The second harmonic generation efficiency of title compound is 2 times that of KDP.

Keywords: NLO crystal; HOMO-LUMO analysis; Dielectric material; Factor group analysis.

Introduction

Currently NLO materials have high potential application and pioneer finding in field of optical computing, optical signal processing, optical communication and dynamic image processing [1-2]. Based on the need of high second order optical non linearity, stable physico-chemical property and stable transparency cut off, high quality NLO crystal has grown in the last few decades. A Different variety of organic, inorganic and semi-organic materials and their molecular systems have been investigated for NLO activity. Due to high order electronic susceptibility structure modification through standard synthetic method, fast response time, organic NLO materials are having a great deal of attention over inorganic NLO materials [4].

Extended π -conjugated systems, the existence of the asymmetrical charge transfer, organic compounds have a high order of non-linearity. Electron donating and electron accepting property of aromatic ring substituent are the reasons for charge transfer [3]. Derivatives of 8-hydroxyquinoline are familiar

compounds for their antibacterial and antifungal activities [5].

Several 8-hydroxyquinoline derivative organic crystals reported for their NLO properties, such as 8-hydroxyquinolinium hydrogen maleate [6], 8-hydroxyquinolinium picrate [7], 8-hydroxyquinolinium dibenzoyl-(L)-tartrate methanol monohydrate [8], 8-hydroxyquinolinium succinate [9], 8-hydroxyquinolinium [10] are worthwhile to mention for their excellent NLO properties. In this article we have reported synthesis, optical property, spectroscopic, thermal and dielectric studies of 8HQB to understand the suitability towards the utilization in opto electronic devices.

Materials and Methods

8-hydroxyquinolinium benzoate was obtained by slow evaporation solution growth method at room temperature using ethanol as solvent. Analytic grade of 8-hydroxyquinoline and Benzoic acid were taken in stoichiometric amounts of 1:1 molar ratio The separate solution of reactants was prepared, mixed by magnetic stirrer and was stirred continuously for about 4 hours the pH value of the solution is 4. The

homogeneous solution was filtered by grade one Whatman filter paper and kept in an airtight container and maintained at a constant temperature to yield good quality of crystal at dust free atmosphere.

The grown 8HQB crystals were characterised by powder X-ray diffraction (XRD) analysis using BRUKER, GERMANY (D8 Advance) X-ray diffractometer with Cu K α radiation. The scanning rate of the sample is in the range of 10-80°. The FTIR spectrum of the 8HQB crystal was recorded in the spectral range 400-4000cm⁻¹ by using a SHIMADZU spectrophotometer. By a Bruker RFS 100/s FTRaman instrument, Raman spectrum was recorded in the region 4000-400 cm⁻¹. ¹H NMR of the 8HQB has been obtained with a Bruker AVANCE III NMR spectrometer operating at 500 MHz with CdCl₃ as a solvent.

UV-Vis absorption spectrum for the titled crystal was recorded with a Lab India UV-Vis spectrophotometer in the wavelength range 200-1100 nm at room temperature. The Thermogravimetric analysis of the grown crystal was carried out using NETZSCH Thermal analysis system between 30 to 500°C. Dielectric studies for 8HQB was carried out using an LCR meter which was used to measure various dielectric parameters like dielectric constant, dielectric loss (tan δ) of grown crystal as a function of various temperature (313, 323, 333 & 343K) and frequency (in the range (100 Hz - 5 MHz). Good samples of 8HQB crystals were electroded after polished by fine grade alumina powder (0.1 μ m).

The intermolecular charge transfer from the end-capping electron-donor to the efficient electron acceptor group through π -conjugated path is highly significant for ascribing the HOMO-LUMO separation. In an electric field $E_i(\omega)$, the nonlinear response of an isolated molecule can be constituted as a Taylor expansion of the total dipole moment μ_t induced by the field.

$$\mu_t = \mu_o + \alpha_{ij} E_i + \beta_{ijk} E_i E_j + \dots$$

Where μ_o is the permanent dipole moment, α_{ij} is linear polarizability and β_{ijk} are the first order hyperpolarizability tensor components.

The component of first order hyperpolarizability can be determined using the relation

$$\beta_i = \beta_{ijk} + \frac{1}{3} \sum (\beta_{ijj} + \beta_{jij} + \beta_{jji}) \dots \dots (2)$$

The total static dipole moment and first order hyperpolarizability tensor of 8HQB, can be calculated by the following equations.

$$\mu_1^0 = (\mu_x^2 + \mu_y^2 + \mu_z^2)^{1/2} \dots \dots (3)$$

$$\beta_{total} = (\beta_x^2 + \beta_y^2 + \beta_z^2) \dots \dots (4)$$

The first order hyperpolarizability from GAUSSIAN 98 W output is given as follows.

$$\beta_{tot} = [(\beta_{xxx} + \beta_{xyy} + \beta_{xzz})^2 + (\beta_{yyy} + \beta_{yzz} + \beta_{yxx})^2 + (\beta_{zzz} + \beta_{zxx} + \beta_{zyy})^2]^{1/2} \dots \dots (5)$$

The calculated values of hyperpolarizability are given in terms of electrostatic units (1 a.u. = 8.639418X10⁻³³ esu). Hyperpolarizability is a third rank tensor; it strongly depends on basis set and the method. Before calculating the hyperpolarizability, the crystallographic data of 8HQB compound was optimized in the UHF (unrestricted open-shell Hartree-Fock) level. The basis set used for calculating the first order hyperpolarizability (β_{ijk}) of 8HQB is B3LYP /6-31G (d,P) by the finite field method using GAUSSIAN 98 W software. The vibrational modes of 8HQB crystals are determined by using Factor group analysis. The second harmonic generation efficiency of the grown crystals is obtained by the Kurtz powder technique. The crystalline sample of 8HQB was ground into very fine powder and tightly packed in a micro capillary tube. A Q-switched Nd:YAG laser working at 1064 nm and 8 ns pulse width with an input repetition rate of 10 Hz and input energy 4.8 mJ/pulse was made to fall on the sample cell. KDP used as the reference material for the SHG analysis of 8HQB.

Results and Discussion

The 8-hydroxyquinolinium benzoate was obtained by slow evaporation solution growth method at room temperature ratio using ethanol as solvent. Good quality of crystal was grown after 20 days of time and the grown crystals of 8HQB are shown in fig. 1. The product was recrystallized twice to remove the impurities. The reaction scheme of 8HQB is given in fig. 2.

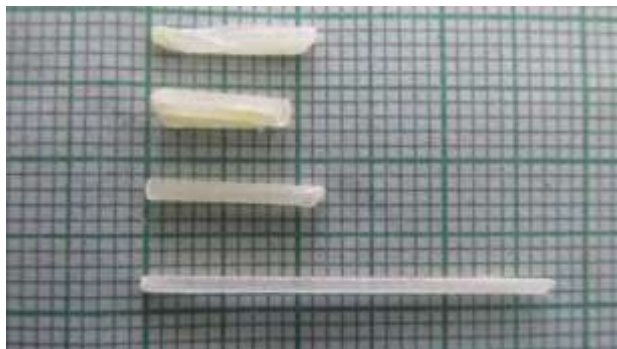


Fig. 1. Grown crystal of 8HQB

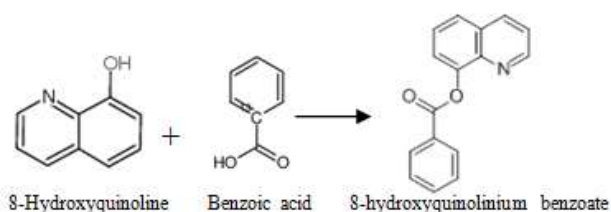


Fig. 2. Scheme of reaction of 8HQB

The powder X-ray diffraction pattern of 8HQB is shown in fig. 3. Prominent peaks in the powder X-ray diffraction confirmed the good crystallinity of the grown crystals. The crystal

structure of 8-hydroxyquinolinium benzoate is monoclinic with centro-symmetric space group $P2_1/c$. The X-ray diffraction peaks were indexed for the lattice parameters $a=6.6322(3) \text{ \AA}$, $b=8.5401(4) \text{ \AA}$, $c=21.5578(10) \text{ \AA}$, $\beta=92.798(1)^\circ$. The lattice parameters obtained in powder X-ray diffraction well suited with the literature [11] and well matched with single crystal X-ray diffraction.

FTIR spectrum of 8HQB is shown in fig. 4. FTIR Raman Spectrum for the titled compound is shown in fig. 5. Frequencies of bending and stretching vibrations, force constant of the donor - acceptor group can be altered by hydrogen bonds. The exact position of the OH band is due to the strength of hydrogen bonds. Intermolecular hydrogen bond between C-O group and O-H group can be presented between 1600 and 1700 cm^{-1} . The ring carbon-carbon stretching vibrations take place in the region between 1625 and 1430 cm^{-1} [12].

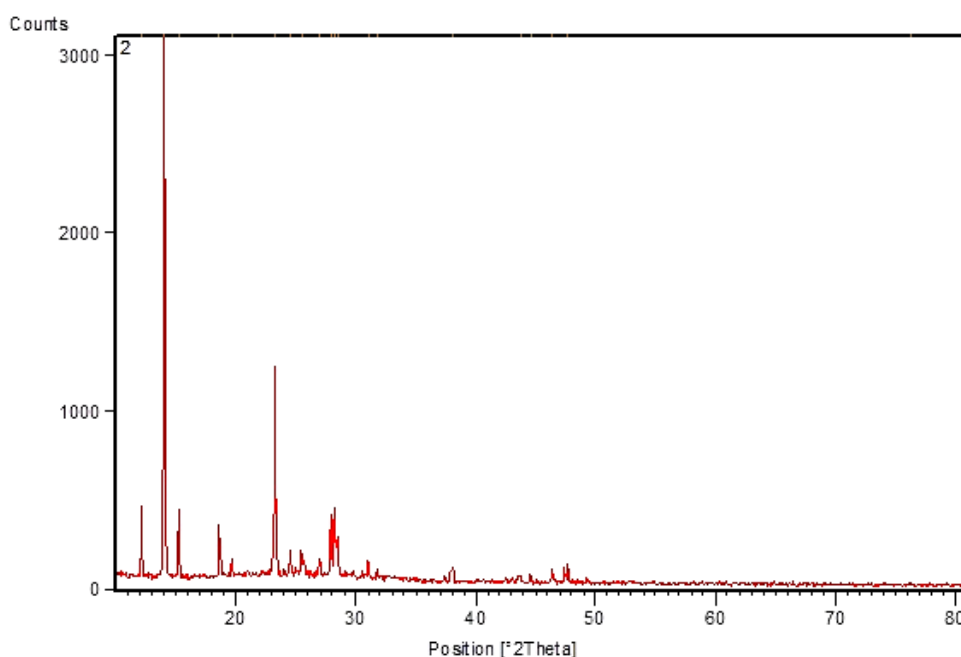


Fig. 3 Powder X-ray diffraction spectrum of 8HQB

The medium intensity vibrational band is observed at 1573 cm^{-1} and its Raman counterpart is appeared at 1582 cm^{-1} , due to carbon-carbon stretching mode. The weak absorption band appeared at 1905 cm^{-1} is attributed as the overtone or combination band due to the C-H out of plane deformation vibration. The identification of vibrational modes at 1388 cm^{-1} in FTIR and 1380 cm^{-1}

FTIRaman is due to CH_2 deformation and represent the ring stretching vibrations of quinoline. The in-plane bending vibrations of quinoline were reported between 750 and 500 cm^{-1} [13]. 723 and 715 cm^{-1} are the vibrational frequencies observed in FTIR and FTIRaman respectively represents the position of in-plane bending vibrations of quinoline.

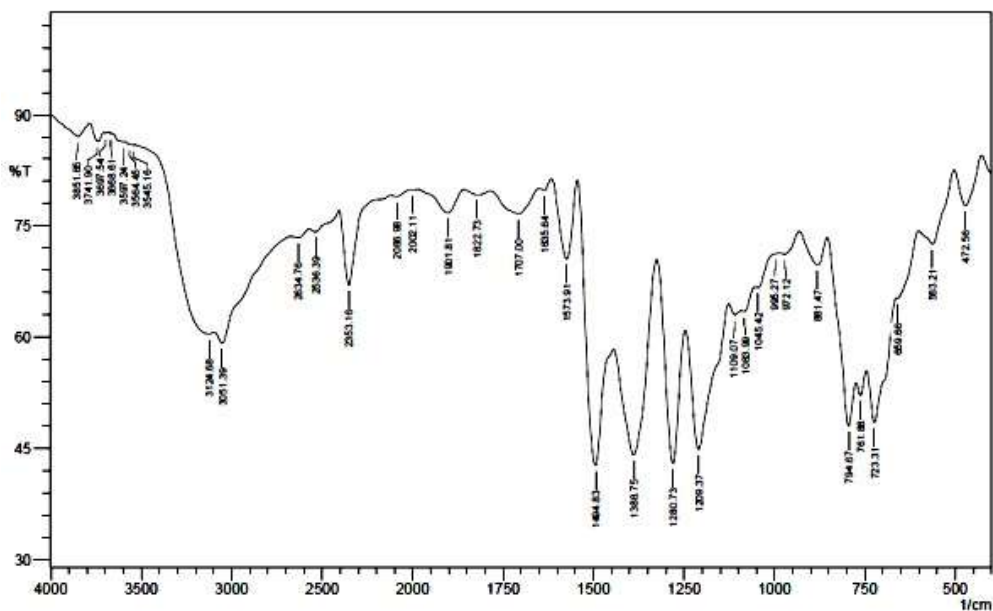


Fig. 4. FTIR spectrum of 8HQB

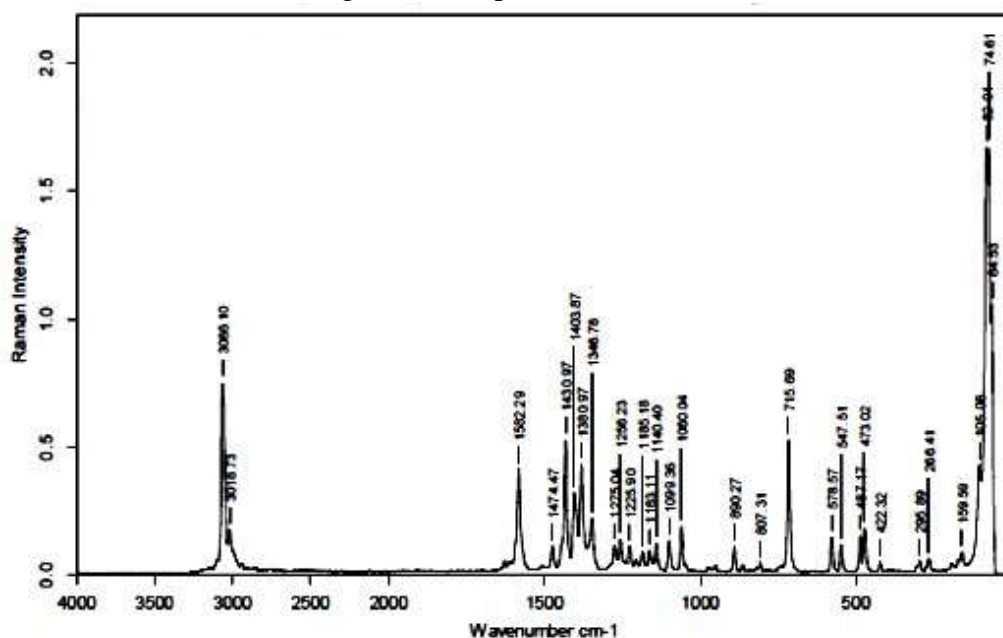


Fig. 5. FTRaman spectrum of 8HQB

Absorption bands appeared at 3051 and 3066 cm^{-1} have been assigned for the C-H stretching mode of 8HQB in FTIR and FTRaman respectively. Vibrations resulting due to C-H in-plane and out of plane C-H bending are found throughout the region 1300-100 cm^{-1} and 900-650 cm^{-1} . In FTIR, these bands give an significant information about the type of aromatic substitution. 881, 794, 723 and 890, 807, 715 cm^{-1} are the absorption band for C-H out of plane bending in FTIR and FTRaman respectively. C-H in plane bending is confirmed by the absorption peak at 1280, 1085 and 1045 cm^{-1} in FTIR spectrum and also the same functional groups are confirmed by the

FTRaman spectrum at 1275, 1099 and 1060 cm^{-1} . The vibrational frequencies and corresponding functional group assignments are tabulated in table 1.

The ^1H NMR spectrum of 8HQB is shown in fig. 6. In proton NMR, missing of the signal near in 10-12 ppm related to protons of carboxylic acid (-COOH) and peak at 5 ppm for hydroxyl substitution in quinolinium confirms the formation of new compounds. It could affirm the formation of the title material via the carboxylic acid deprotonation. A doublet exhibited at 8.77 and 8.15 ppm represents the position of protons in 8-hydroxyquinoline and benzoate moieties respectively. A $\delta=7.47, 7.43,$

7.40, 7.33 ppm peaks represent the position of protons at 8-hydroxyquinoline moiety. At $\delta=7.45, 7.32, 7.18$ ppm owes to the position of protons in the benzoate moiety.

As a NLO material, remarkable parameters for a single crystal utilised in optical applications and Opto electronic device fabrication are the range of optical transmittance and the transparency cut off [14]. The lower cut off wavelength for 8HQB crystal is 243 nm and 65% transmittance observed over a frequency range from 400 to 800 nm. The low percentage of transmission can be ascribed to purity of starting material and growth method. The convincing evidence of this result is obtained from transmission spectrum, is shown in fig. 7 and it indicates that the grown 8HQB material can be used in NLO applications.

Table 1. Vibrational frequency and band assignments of 8HQB

Wavenumber, cm^{-1}		Vibrational band assignments
FTIR	FTRaman	
3051	3066	C-H stretch
1573	1582	-C=C- stretch
1494	1474	Ring stretch
1388	1380	C=O sym stretch
1280	1275	C-H in plane
1209	1225	C-H in plane
1083	1099	C-H in plane
1045	1060	C-H in plane
881	890	C-H out of plane
794	807	C-H out of plane
472	473	Out of plane ring bending

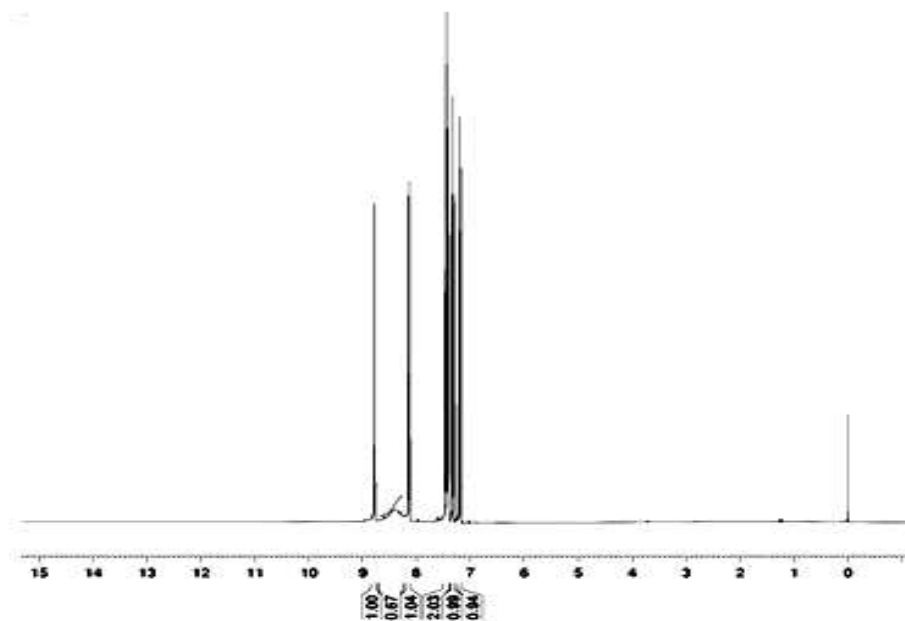


Fig. 6. ^1H NMR spectrum of 8HQB

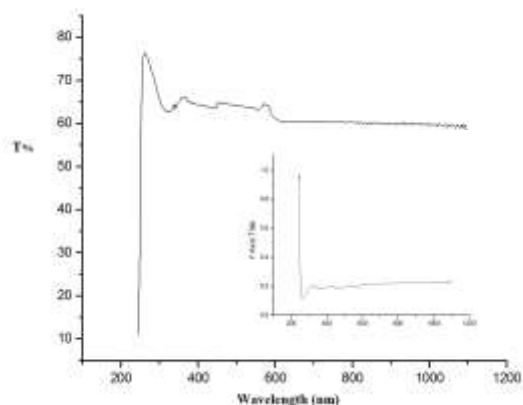


Fig. 7. Transmittance spectrum of 8HQB

The TG and DTA traces are shown in fig. 8. There is a major weight loss that starts at 80°C and propagated up to 250°C . The clear endotherm peak at 80°C could be ascribed to melting point of 8HQB crystal. A good degree of crystallinity and purity of the material was ascertained by the sharpness of the peak [15]. The melting point of 8HQB crystals was also verified using a melting point apparatus. The temperature of the powder sample of 8HQB was gradually increased and the material starts to melt from 80°C into and converted into a transparent solution. The result reveals that the

maximum temperature for NLO applications of 8HQB is limited up to 80°C.

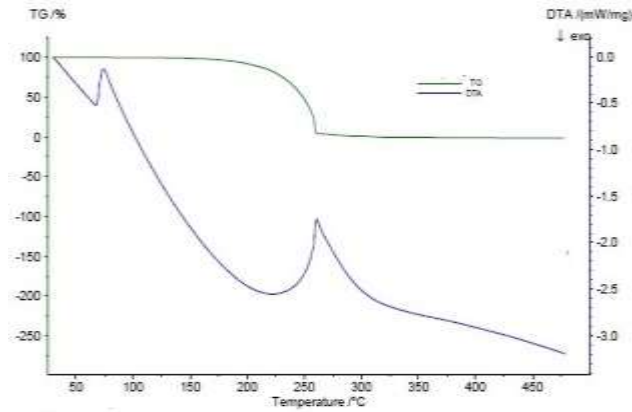


Fig. 8. TG/DTA analysis of 8HQB

The reduction of the dielectric constant with the increase in the frequency may be because of the nature of the dipoles in material to align along the field direction [16]. Due to the non-debye behaviour the dielectric constant varies with frequency in 8HQB can be ascribed to the constitution of the space charges at the electrode and crystal interface [17]. Decreases of dielectric constant at high frequencies in 8HQB crystals may be due to the fast periodic reversal of the electric field occurs, thus the polarization due to reduction of accumulation of charges of interfaces of crystal and electrode [18]. Inactiveness of space charge polarization at lower frequencies and high temperature confirms the sign of perfection of crystal [19]. Fig. 9 shows the variation of dielectric constant of 8HQB as a function of temperature and frequency. The dielectric constant of 8HQB was calculated using the relation

$$\epsilon_r = \frac{Ct}{\epsilon_0 A} \dots\dots\dots(1)$$

where ϵ_0 is the permittivity of free space, t is the thickness of the sample; A is the area of a cross section of the grown crystal of 8HQB.

Variation of dielectric loss with frequency and temperature of 8HQB is given in fig. 10. At lower frequencies, the higher value of dielectric loss is due to the “free” charge build up at the electrode–crystal interface [20]. Before the electric field is reversed at low frequencies there is enough time for accumulation of the charges and this may cause to the large value of dielectric loss in the material. At high frequency there is no time for the accumulation of the charges at the interface. The charges ramp up at the boundaries of conducting species in the

material. This process leads to the so-called “conductivity relaxation” [21,22].

Dielectric loss

$$\tan \delta = D\epsilon_r \dots\dots 2$$

where, ϵ_r is the relative permittivity of the crystal and D is dissipation factor.

Reduction of space charge polarization in high frequency may increase the conductivity of dielectric material for a given temperature which confirms the small polaron loss in the 8HQB crystal. A.C conductivity behaviour of 8HQB with frequency is shown in fig. 11.

$$\sigma_{ac} = 2\pi f \epsilon_0 \epsilon_r \tan \delta \dots\dots\dots 3$$

where $\epsilon_0 = 8.854 \times 10^{-12} \text{ Fm}^{-1}$, f is the frequency of the applied dielectric field, ϵ_r the dielectric constant and $\tan \delta$ is the dissipation factor.

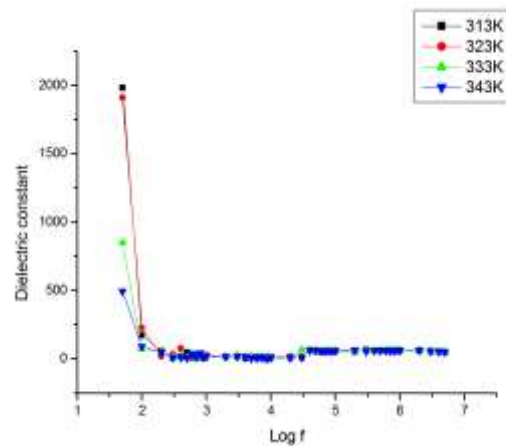


Fig. 9. Variation of Dielectric constant with frequency

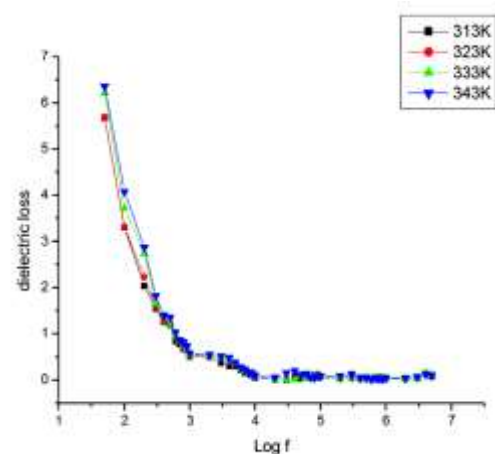


Fig. 10. Variation of dielectric loss with frequency

The HOMO is the orbital that behaves as an electron donor and the LUMO is the orbital that behaves as the electron acceptor. Portending

the most reactive position in π -electron system and various types of reaction in the conjugated system was explained by the molecular orbital and their properties like energy [23]. The energy gap between HOMO and LUMO evaluate the optical kinetic stability, chemical hardness, polarizability and chemical reactivity [24]. The cell parameter discloses that the π - π^* transition which gives rise to the NLO properties of the 8HQB crystal.

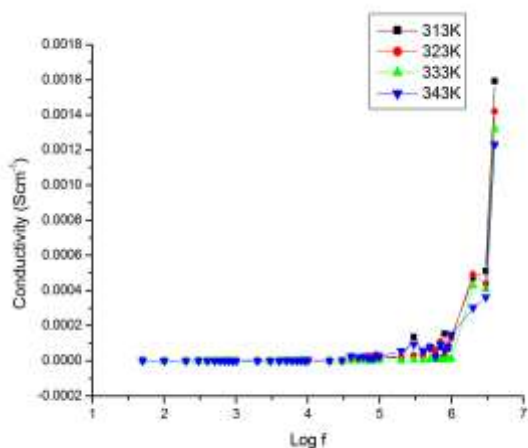


Fig. 11. Variation of conductivity with frequency

The calculated values of first order hyperpolarizability of 8HQB is $3.88823E^{-30}$ (esu) and the dipole moments are $\mu_x=0.3284842$, $\mu_y=-0.190385$, $\mu_z=-0.6148271$ and $\mu_{total}=-0.4767279$. Domination of particular hyperpolarizability component (β_{xxx}) indicates on a significant delocalization of charges in those directions. The calculated hyperpolarizability values of 8HQB are tabulated in table 2. The higher dipole moment values are associated with larger projection of β_{total} quantities. The connection between the dipole moments and first order hyperpolarizability of organic molecules are widely recognized in the literature [25]. The lowering the value of energy gap between this orbital explains the charge transfer interactions occur within the organic molecule and reveals the chemical activity. The HOMO-LUMO plots of 8HQB are shown in fig. 12.

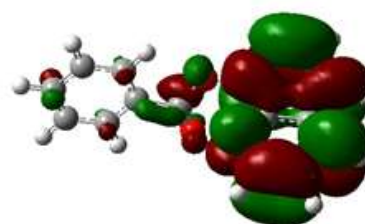
The vibrational modes of 8HQB crystals are determined by using Factor group analysis method based on the procedures outlined by Rousseau et al [26]. The 8HQB crystal crystallized in the monoclinic system, $P2_1/c$ space group, the C_2 point group and molecule has 30 atoms ($Z=4$). The total vibrational mode of

8HQB crystal is 360. The total vibrational modes are decomposed according to the irreducible representation of the point group as $\Gamma_{total}=90A_g+89A_u+90B_g+88B_u$ and $\Gamma_{acou}=A_u+2B_u$. Three acoustic modes represent the translations of free molecule, which leads to inactive Infrared (IR) mode in the crystal. The total vibration modes predict 336 internal vibrations which can be distributed as $(84A_g+84A_u+84B_g+84B_u)$ and 24 external modes such as $(3A_g+3A_u+3B_g+3B_u)$ translational, $(3A_g+3A_u+3B_g+3B_u)$ vibrational modes. The results of the factor group analysis are given in table 3.

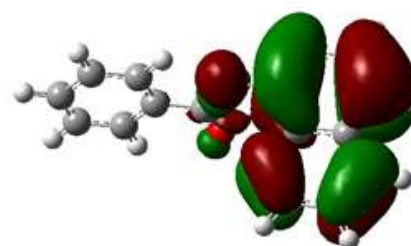
Table 2. First order hyperpolarizability of 8HQB derived from DFT calculation

β	values
β_{xxx}	196.7084349
β_{xxy}	-83.0793172
β_{xyy}	182.5762149
β_{yyy}	-373.7081334
β_{xxz}	37.354757
β_{xyz}	-22.6351786
β_{yyz}	10.0435313
β_{xzz}	-43.5056477
β_{yzz}	74.2539956
β_{zzz}	11.4616133
$\beta_{Total, au}$	450.0574269
$\beta_{Total, esu}$	$3.88823E-30$

LUMO



HOMO



$\Delta E=0.016a.u$
B3LYP/6-31G (d,P)

Fig. 12. HOMO-LUMO plot of 8HQB

Table 3. Factor group analysis of 8HQB

Factor Group symmetry	Site symmetry		$C_{16}H_{11}NO_2$ Compound								
	Total Vibrations		C	H	N	O	Total mode	Optical mode	Acoustic mode	Activity	
	Internal mode	External mode								IR	Raman
A_g	84	3T,3R	48	33	3	6	90	90	--	R_z	$\alpha_{xx}, \alpha_{yy}, \alpha_{zz}, \alpha_{xy}$
A_u	84	3T,3R	48	33	3	6	90	89	1	T_z	--
B_g	84	3T,3R	48	33	3	6	90	90	--	R_x, R_y	α_{xz}, α_{yz}
B_u	84	3T,3R	48	33	3	6	90	88	2	T_x, T_y	--
Total	336	24	192	132	12	24	360	357	3		

The second-harmonic generation (SHG) is a cognitive process to new laser technology and for the electro-optic effect. A quantitative analysis of the second harmonic generation efficiency of 8HQB crystal was determined by Kurtz powder technique [27]. The grown crystal of 8HQB crystallized in a $P2_1/C$ space group with crystal system of monoclinic in centrosymmetric manner. The induced SHG is observed and not intrinsic. Some of the crystals even grown in centrosymmetric space groups [28] may yield the second harmonic generation due to the presence of defects or internal stress or surface effect and it causes the local breaking of symmetry [29,30]. Based on the fact that the 8HQB crystal also shows the SHG and is 2 times of KDP. Comparable values of SHG for 8HQB and KDP are shown in table 4.

Table 4. Comparison of SHG Value for 8HQB and KDP

Input Energy, mJ/pulse	Output power, mW	
	KDP	8HQB
4.8	78	156

Conclusions

8HQB crystals are grown by the slow evaporation technique using ethanol as solvent and with the molecular complex of 8-hydroxy quinoline and benzoic acid (1:1). The crystal structure of the titled compound confirmed and the lattice parameters have been calculated using X-ray diffraction studies. Various vibrational frequencies are observed using FTIR and FTRaman spectra. 1H NMR studies provided the information about the chemical environmental of title material. The first order hyperpolarizability

(β) of 8HQB crystals was found to be 3.88823E-30 esu using the B3LYP /6-31G (d,P) basis set. The UV-visible spectrum cut-off wavelength is found to be 243 nm. The dielectric behaviour of 8HQB crystal is confirmed from the dielectric studies as the function of temperature and frequency. The thermal stability of 8HQB was affirmed from a sharp endothermic peak in the DTA. The SHG conversion efficiency of 8HQB was found to be two times that of KDP.

Conflicts of Interest

The authors hereby declare that they have no conflict of interest.

References

- [1] Xue D, Zhang S. Nonlinearity of the complex crystals with O-H bond. *J Phys Chem solids* 1995;57:1321-1328.
- [2] Xu D, Xue D. Chemical bond simulation of KADP single-crystal growth. *Journal of Crystal Growth* 2008;310:1385-1390.
- [3] Anandhababu G, Ramasamy P. Investigation of crystal growth, structural, optical, dielectric, mechanical and thermal properties of a novel organic crystal: 4, 4'-dimethylbenzophenone. *Journal of Crystal Growth* 2008;310:3561-3567.
- [4] Vijayan N, Bhagavannarayana G, Murga KK, Pal S, Dutta SN, Gopalakrishnan R, Ramasamy P. Studies on the structural, thermal and optical behaviour of solution grown organic NLO material: 8-hydroxyquinoline. *Cryst Res Technol*. 2007;42:195-200.
- [5] Bambury RE, Wolff M.E (Ed). *Burger's Medicinal chemistry, Part II*, John Wiley, New York. 1979.

- [6] Permaiyan G, Pandi P, Vijayan N, Bhagavannarayana G, MohanKumar R. Crystal growth, structural, thermal, optical and laser damage threshold studies of 8-hydroxyquinolinium hydrogen maleate single crystals. *Journal of Crystal Growth* 2013;375:6-9.
- [7] Krishnakumar V. Nagalakshmi R. Vibrational spectroscopic studies of an organic non-linear optical crystal 8-hydroxyquinolinium picrate. *Spectrochimica Acta Part A*. 2007;66:924-934.
- [8] Sudarsana N, Krishnakumar V. Nagalakshmi R. Experimental and theoretical investigations of non-centrosymmetric 8-hydroxyquinolinium dibenzoyl - (L)-tartrate methanol monohydrate single crystal. *Materials Research Bulletin* 2015;61:136-145.
- [9] Thirumurugan R, Babu B, Anith K., Chandrasekaran. Investigation on growth, structure and characterization of succinate salt of 8-hydroxyquinoline: An organic NLO crystal, *J Spectrochimica Acta Part A*. 2015;14:44-53.
- [10] Prabhakaran SP, Ramesh Babu R, Velusamy P, Ramamurthi K. Studies on the growth, structural, optical, mechanical properties of 8-hydroxyquinoline single crystal by vertical Bridgman technique. *Materials Research Bulletin* 2011;46:1781-1785.
- [11] Lei G. 8-Quinolyl benzoate. *Acta Cryst*. 2006;E62:o4666-o4667.
- [12] Socrates G. *Infrared Characteristic Group Frequencies*, John Wiley, New York. 2000.
- [13] Wait Jr SC, Mc Nerney JC. Vibrational spectra and assignments for quinoline and isoquinoline. *J Mol Spectrosc*. 1970;34:56-77.
- [14] Wang L, Zhang GH, Liu XT, Wang LN, Wang XQ, Zhu LY, Xu D. A novel L-arginine salt nonlinear optical crystal: L-arginine p-nitrobenzoate monohydrate (LANB). *Journal of Molecular Structure* 2014;1058:155-162.
- [15] Willard HH, Merritt Jr LL, Dean JA, Settle Jr FA. *Instrumental methods of Analysis*, Wadsworth Publishing Company, USA, 1986.
- [16] Nada AMA, Dawy M, Salama AH. Dielectric properties and ac-conductivity of cellulose polyethylene glycol blends. *Mater Chem Phys*. 2004;84:205-215.
- [17] Macdonald JR (Ed.). *Impedance Spectroscopy*. Wiley, New York, 1987.
- [18] Ramesh S, Yahaya AH, Arof AK. Dielectric behaviour of PVC-based polymer electrolytes. *Solid State Ionics* 2002;291:152-153.
- [19] Balaji J, Prabu S, Srinivasan P, Srinivasan T, Velmurugan D. Studies on the growth and characterization of a non-linear optical crystal: 3 Hydroxy Pyridinium Tartrate Mono Hydrate (3HPTMH). *Spectrochimica Acta A*. 2015;144:139-147.
- [20] Bozkurt A. Dielectric and conductivity relaxations in quaternary ammonium polymer. *J Phys Chem Solids* 2002;63:685-690.
- [21] Kyrstis A, Pissis P, Grammatikakis J. Dielectric relaxation spectroscopy in poly (hydroxyethyl acrylates)/water hydrogels. *J Polym Sci Part B: Polym Phys* 1995;33:1737-1750.
- [22] Dyre J.C. *J. Non-Cryst. Solid*. 1995;135:219.
- [23] Fukui K, Yonezawa T, Singu H. A molecular orbital theory of reactivity in aromatic hydrocarbons. *J Chem Phys*. 1952;20:722.
- [24] Kosar B, Albayrak C. Spectroscopic investigations and quantum chemical computational study of (E)-4-methoxy-2-[(p-tolylimino) methyl] phenol. *Spectrochim Acta A*. 2011;78:160-167.
- [25] Prasad PN, Williams DJ. *Introduction to Nonlinear Optical Effects. Molecules and Polymers*; Wiley: New York, 1991.
- [26] Roussacau, DL, Bauman RP, Porto SPS. Vibrational Raman optical activity of simple amino acids. *J Raman Spectrosc*. 1993;24:91-96.
- [27] Kurtz S.K. Perry T.T. A powder technique for the evaluation of nonlinear optical materials. *J Appl Phys*. 1968;39:3798-3801.
- [28] Mohd.Shakir SK, Kushwaha KK, Maurya, MA, Bhagavannarayana G. Growth and characterization of glycine picrate—Remarkable second-harmonic generation in centrosymmetric crystal. *Journal of Crystal Growth* 2009;311:3871-3875

- [29] Balaji J, Prabu S, Sajan D, Srinivasan P. Investigations on spectroscopic, dielectric and optical studies in 3-hydroxypyridinium 4-nitrobenzoate crystals. *Journal of Molecular Structure*. 2017;1137:142-149.
- [30] Muthu K, Meenakshisundaram S. Crystal growth, structure and characterization of *p*-Toluidinium picrate. *Journal of Crystal Growth* 2012;352:163-166.
